Hybrid nanostructures with enhanced optical and magnetic properties

Author: Silvia Mena Barrientos, Treball de Fi de Grau
Facultat de Física, Universitat de Barcelona, Diagonal 645, 08028 Barcelona, Spain.

Advisor: Dr. Xavier Batlle, Departament de Física de la Matèria Condensada

Abstract: This is an experimental work where synthesis of both magnetite and gold nanoparticles (NPs) have been performed in the laboratory, obtaining gold NPs with a diameter of 4 nm and magnetite NPs of 8 nm. Afterwards, these NPs were protected following two different methods. First, a silica coating was tried, while the second method was performed with 11-mercaptoundecanoic acid (MUA) both aiming at building a hybrid nanostructure combining both NPs. Finally, to determine the quality and characterization of the resultant nanostructures, several measurements have been done, such as transmission electron microscopy, thermogravimetry, hysteresis loops and absorbance.

I. INTRODUCTION

Nanotechnology has evolved largely during the latter years[1]. The idea of using very small structures has prompted major advances in multiple fields such as materials industry and biomedicine[1]. Working at nano scale offers a lot of advantages in the biology studies and healthcare [1, 2].

In this work, we will focus on the synthesis of nanoparticles (NPs) with interesting properties for biomedicine application. The possibility to build structures where optical and magnetic properties can be highly controlled has increased the interest of nanoparticles in biological systems for diagnostic and therapeutic applications, such as diagnosis of diseases, drug delivery, catalysis and water treatment [3].

Gold nanoparticles systems show potential for diagnostic and therapeutic applications due to the fact that they are easy to produce, have ready bioconjugation, good biocompatibility and unique optical properties. The surface plasmon absorption (SPA) of gold nanostructures is the responsible of their remarkable optical properties. However, these results are highly dependent on the particle surface, size, shape and the medium where the particles are suspended [4]. Gold nanoshells are interesting because they possess strong absorbance with tunable wavelengths from the visible to the infrared region. Noble materials such as gold, a decrease in the size below the electron mean free path implies an increase of the absorption in the visible-near-UV [2]. This property could play an important role in biomedical imaging applications and could be even implemented in localized photothermal therapy [1, 2].

On the other hand, magnetic nanoparticles show other relevant properties that may have significant applications in biomedicine too. These features are superparamagnetism - they only respond in the presence of a magnetic field [5]-, high field irreversibility, high saturation field, extra anisotropy contributions or shifted loops after field cooling [1].Iron oxide particles such as magnetite, Fe_3O_4 are by far one of the most commonly used for biomedical application.

As optical and magnetic properties at nanometer scale are very useful for biomedicine application, multifunctional nanoparticles possessing both properties have gained the attention of the scientific community and building hybrid multifunctional nanostructures have been attempted [2, 4].

Following this last idea, we have tried to build a multifunctional hybrid nanostructure. In this TFG, the synthesis and characterization of 4 nm gold and 8 nm magnetite nanoparticles is described. Also, it is presented a silica coating of magnetic particles. Finally, with the aim to enhance optical and magnetic properties of both nanostructures, a hybrid nanostructure combining magnetite and gold particles was attempted.

One point that has to be taken into account when performing synthesis procedures is that in order to make the NPs biocompatible they must be transformed into water-soluble NPs by changing the surfactant ligands. For this reason, silica coating and the hybrid nanosctructure have to be performed in aqueous media [6]

II. EXPERIMENTAL SECTION

A. Sample preparation

a. Materials In order to succeed in the synthesis, the following reactants and dissolvents were used: iron(III) acetylacetonate ($Fe(acac)_3$) (Sigma-Aldrich, $\geq$ 99%), oleic acid (Sigma-Aldrich, 90%), 1,2-hexadecanediol (Sigma-Aldrich, 90%), 1-octadecene (Sigma-Aldrich, 90%), acetone (Sigma-Aldrich,99%), hexane (AppliChem Panreac ITW Companies, 95%), ethanol (AppliChem Panreac ITW Reagents, 96%), methanol (Panreac, 99.8%), cyclohexane (Sigma-Aldrich, 99.5%), IGEPAL CO-520 (Sigma-Aldrich), amonium hydroxide solution (Sigma-Aldrich), tetraethyl orthosilicate (TEOS) (Sigma-Aldrich), (3-aminopropyl)triethoxysilane (APTES) (Sigma-Aldrich, 99%), gold (III) chloride hydrate (Sigma-Aldrich, 99.999%), sodium citrate (Sigma-Aldrich), sodium borohydride (Sigma-Aldrich, $\geq$96%), 11-mercaptoundecanoic

acid (MUA) (Sigma-Aldrich, 95%), chloroform (Fluka, $\geq$ 99.8%). All chemical were used as recieved, without further purification.

b. Magnetite NPs The followed procedure was based on refs [7, 8], with some modifications. 0.36 g of $Fe(acac)_3$, 1.15 g oleic acid, 1.5 g of 1,2-hexadecanediol were mixed in 20 mL of 1-octadecene. The reaction was heated up with a rate of 21 ^{o}C/min until it reached 105 ^{o}C and kept at this temperature for 30 min vacuum. Then, it was reheated up to 200 ^{o}C with a rate of 3.16 ^{o}C/min and kept at constant temperature for 2 h. Then, the temperature was risen to 310 ^{o}C with a 11 ^{o}C/min rate and maintained at this point for 1 h. All the procedure was under an argon atmosphere and vigorous magnetic stirring (1100 rpm). Afterwards, the solution was cooled down to room temperature and washed with a mixture of hexane and acetone with 1 : 3 volume ratio. To make the NPs precipitate, the mixture was centrifuged during 10 min at 9000 rpm. This washing procedure was repeated at least three times, to be sure that the supernatant was clear. Finally, the precipitate was decanted and then redispersed in toluene. Fe_3O_4 NPs of 8 nm were obtained.

c. Gold NPs Our synthesis was based on ref [3]. 1 mL of $HAuCl_4$ 1 % (0.04M) was mixed with 100 mL of deionized water at room tempeature. Then, 2 mL of sodium citrate 1 % (0.04 M) solution were added and, also, 1 mL of fresh 0.075 % sodium borohydride in 1 mL of sodium citate 1%. The solution was stirred for 10 min. Finally, Au NPs of 4 nm were obtained.

d. Silica coating In order to contain Fe_3O_4 nanoparticles in aqueous media, a silica coating was added following the microemulsion method. For a sample of 5 mg of Fe_3O_4 NPs dispersed in cyclohexane, 0.8 mL of IGEPAL CO-520 were mixed with 15 mL of cyclohexane and stirred 1 min with ultrasounds. Then, 5 mg of NPs were added and the mixture was mechanically stirred for 30 min. After that, 0.130 mL of NH_4OH 30 % were added to the solution, 15 more minutes at the mechanical stirring. Then 0.15 mL of TEOS were added and the mixture was left to mechanical stirring for 22 h. Afterwards, it was washed following a two steps procedure, the first wash was with methanol, the mixture was left 1 min in vortex stirring and then, 5 min with ultrasounds and centrifuged 10 min at 9000 rpm. These steps were repeated twice. The second part was all the same but changing methanol with ethanol and, again, made for three times. Finally, the precipitate was dispersed in H_2O [9].

e. Hybrid nanostructure with MUA The procedure followed was based on ref [6] with some modifications. 2 mg of Fe_3O_4 NPs were dispersed in 1 mL of cyclohexane. Then, 0.1 g of MUA were added and finally, 2 mL of $CHCl_3$ as a solvent. Afterwards, the solution was left with mechanical stirring for 48 h. Then, $CHCl_3$ was used to make a first wash and centrifuged at 9000 rpm for 10 min. A second wash was made with ethanol and the mixture was again centrifuged under the same conditions. Finally, the Fe_3O_4 NPs were dispersed in deionized water. After that, 5 mL of gold NPs in aqueous media were added and the mixture was mechanically stirred overnight. The following day, the solution was washed with H_2O and centrifuged for 10 min at 9000 rpm. Finally, the precipitate was redispersed in deionized water.

B. Experimental techniques

a. TEM With the aim to determine the shape and size of the NPs, micrographs were taken with transmission electron microscope (TEM) using a JOEL 1010 100 kV. For its characterization, samples were dropped onto a carbon-coated grid and dried in oven. To obtain the mean size at least 2,000 particles were measured for each sample using ImageJ software. Then, size distributions were fitted to a log-normal function.

b. TGA With thermogravimetric analysis (TGA) the organic fraction of the coating of the magnetite NPs was studied. To obtain these measurements, TGA-SDTA 851e/SF/1100 (Mettler Toledo) was used at a heating rate of 10 ^{o}C min^{-1} with a nitrogen atmosphere from room temperature up to 800 ^{o}C.

c. Magnetic characterization The magnetization measurements of magnetite NPs were performed in powder state, using a Quantum Design SQUID magnetometer. Hysteresis loops, M(H) were recorded at 5 K and 300 K under a $\pm$ 50 kOe (1 Oe = 79.57747 A/m) as a maximum value of the magnetic field to determine the saturation magnetization, M_s, which can be defined as the magnetization when all the particle moments become aligned along the external applied magnetic field, and coercive field, H_c, which is the reversed magnetic field applied to cancel the sample magnetization. The measured values were recalculated by subtracting the organic fraction obtained by TGA. Moreover, in order to study the dependence of magnetization with temperature, field cooling (FC) and zero field cooling (ZFC) methods were followed. ZFC measurements starts with cooling down the sample from room temperature to 5 K in zero magnetic field. After that, a static magnetic field is applied ($H<<H_c$), while temperature is increasing and M_{ZFC} is measured. When room temperature is reached, the sample is cooled down again with the field applied and then, it is reheated up to 300 K, while M_{FC} is measured under the same magnetic field [10].

d. Optical characterization A V-550 spectrophotometer was used to obtain the UV-vis spectra.

III. RESULTS AND DISCUSSION

a. Characterization of magnetite NPs From TEM images Fig.1 one can distinguish small and almost spherical particles separated a few nanometers. In this case, the magnetite NPs have an average diameter of 8.0 nm

with σ = 1.8 and a relative standard deviation, RSD = 23%. In the histogram it is noticeable that the size dispersion of the NPs could be approximated to a log-normal behaviour. With TGA analysis it was concluded

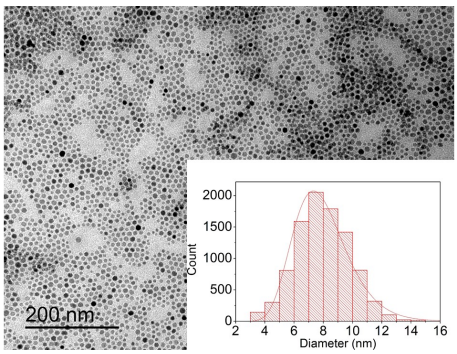

FIG. 1: TEM image of magnetite NPs and the histogram of size distribution, fitted to a log-normal distribution.

that the studied sample was 74% magnetic. Within this method all the weigh-loss corresponds to the evaporated water and all the oleic acid that was in the sample. Once knowing the magnetic proportion of the magnetite NPs, and after having applied it to the hysteresis loops, results are shown in Fig.2. One can determine for each temperature the values of M_s and H_c. At 300 K, we got a M_s = 75 emu/g with no coercive field, suggesting that the NPs are superparamagnetic. While, at 5 K both values increase, M_s = 92 emu/g and H_c = 305 Oe. This M_s value is really close to that of the bulk magnetite, 98 emu/g at 5 K [8], which is a very satisfying result as is an almost perfect bulk-like ferrimagnetic order.

Fig.3 shows the thermal dependence of magnetization where ZFC and FC measurement were done. From the ZFC curve, a maximum of magnetization was achieved at 75 K, this peak corresponds to the blocking temperature, point where the majority of the particles become aligned with the magnetic field since they are transiting between the block and superparamagnetic state. Once this temperature is reached, the curve decreases again because of thermal excitation. However, this peak is not present in the FC curve, as during the field cooling process there is a progressive alignment of the particle moments along the direction of the magnetic field [10]. At temperatures above the peak, both curves follow a similar behaviour. Also, it has to be mentioned that one possible reason why both curves do not coincide in the maximum might be due to dipole-dipole interactions as the measurements were performed in powder state. This phenomena would not be related to a bad polidispersion of the sample, as with TEM images we concluded that was very good.

b. Characterization of gold NPs Fig.4 presents a TEM image of Au NPs, as compared to magnetite in Fig. 1, shows that while gold particles are smaller, the distances kept between particles are larger. In this case, the average diameter of gold NPs was 4.4 nm with σ = 1.1 and a RSD = 25 %. Moreover, as in the magnetite

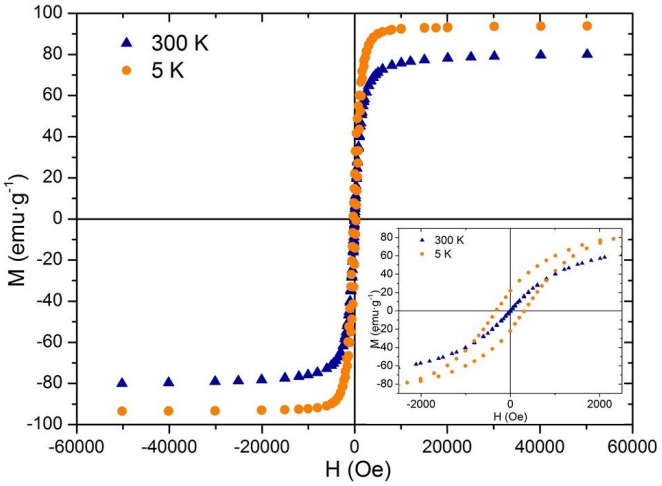

FIG. 2: Hysteresis loops at 5 K and 300 K with an iinset at the low-field region to evaluate the coercive fields.

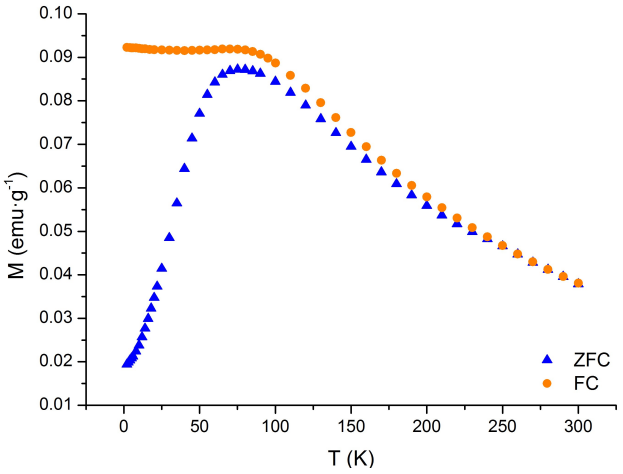

FIG. 3: Magnetization as a function of temperature at field cooling and zero field cooling procedures.

case, size distribution follows a log-normal distribution function.

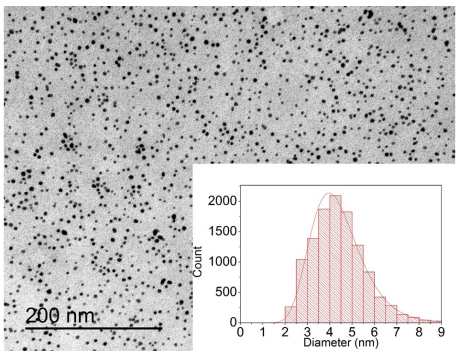

FIG. 4: TEM image of gold nanoparticles and the histogram of size distribution, fitted to a log-normal distribution.

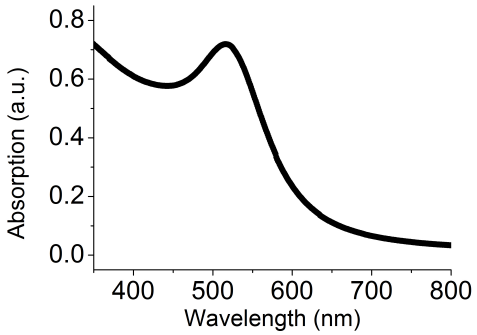

FIG. 5: Normalized UV-vis spectra of gold nanoparticles.

Fig.5 shows the UV-vis absorption spectra of gold nanoparticles. There is not absorption for large wavelength values, whereas it is in the visible region where NPs increase its absorbance due to the plasmons from the surface. The maximum peak is as expected at ~ 515 nm, which is the manifestation of surface plasmon resonance [11]. This result is coherent with others from the bibliography consulted [2, 3, 11]. Moreover, in the near UV there is an interband transition where electrons from 5s band, which is semi-filled, move to superior bands. Thus, it can be assumed that the synthesised NPs have high absorption values below 600 nm, then, the values absorbance starts to decrease.

c. Silica coating As synthesized, nanoparticles are surrounded by oleic acid so are only dispersible in organic media. To have them in aqueous media, a silica coating is used. In Fig.6(a) a core-shell can be easily distinguished; in the middle, the magnetite nanoparticle (the darker core) covered by the silica coating (with a lighter contrast) with $\sim$ 10 nm thickness. This procedure was quite a success as the coating attached well to the nanoparticles. Comparing Fig.6(a) to Fig.1, it can be seen that the addition of the silica attachment was well performed and does not cause much aggregation, whereas if we now focus on Fig.6(b), where there is a silica coating from the same NPs sample with APTES (with a NH_3 group that presents affinity to gold nanoparticles), high aggregation is shown. For this reason, we decided to try with another method to build the hybrid nanostructure.

d. Hybrid nanostructure with MUA Finally, MUA was used with the aim of building a hybrid nanostructure combining gold and magnetite nanoparticles. MUA was chosen to perform the exchange ligands of both nanoparticles due to its molecular structure contains the functional groups, SH- and COOH- as seen in Fig.7, which are capable to link with Au and Fe_3O_4, respectively. On one hand, MUA, with its carboxylic group (COOH-) would work as an exchange ligand for magnetic nanoparticles displacing the oleic acid with the aim to disperse the particles in water, where gold was dispersed too. While, on the other hand, MUA has a thiol group (-SH) in one end of the molecule to which gold particles present a high

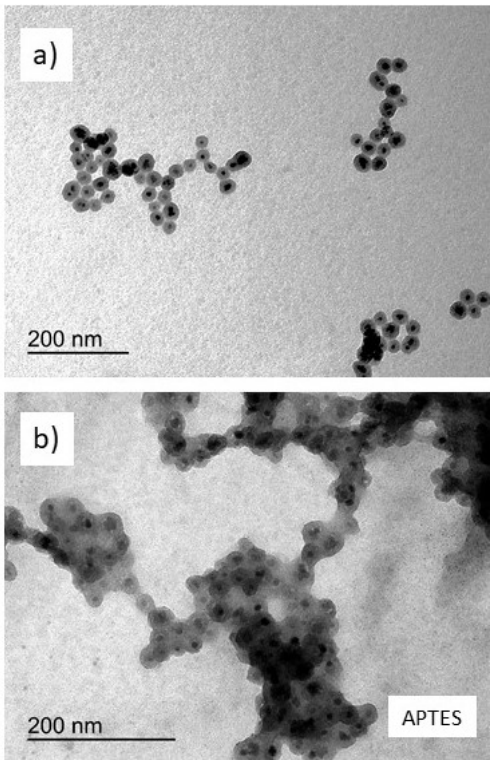

FIG. 6: (a) Silica coating attached to magnetite NPs without APTES, (b) with APTES, both from the same NPs sample.

affinity, so it was thought that MUA would be a good ligand exchange with gold nanoparticles too [5]. In Fig.8, two images of the process are shown. Initially the magnetic NPs were combined with the MUA and, once the ligand exchange was performed, gold nanoparticles were added, obtaining the hybrid nanostructure. However, focussing on the images, it can be seen that the addition of MUA to the magnetite structures, increase its aggregation compared to the previous solution with only magnetite. One possible explanation might be the formation of S-S bonds which would make complex the link with gold NPs as there would be less SH free. This fact might be another reason why the aggregation grew when gold particles were added. In Fig.8(b) it is very difficult to distinguish the different combined nanostructures.

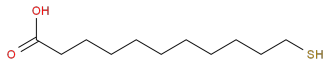

FIG. 7: Chemical structure of MUA.

IV. CONCLUSIONS

In this work, the synthesis procedure of both magnetic and plasmonic nanoparticles was successful. The procedure has been repeated several times and the results have

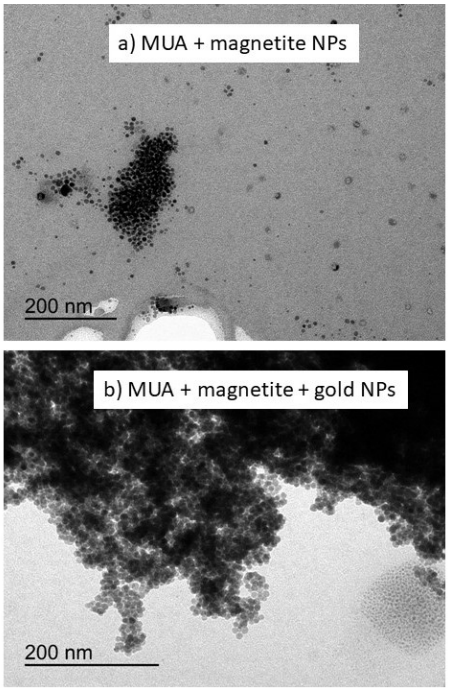

FIG. 8: TEM images of (a) MUA combined with magnetite, (b) MUA combined with gold and magnetite NPs.

shown similar characterization. Moreover, the characterization was very satisfying as the magnetite NPs have high magnetization and gold particles have the expected absorbance spectra. The attachment of silica coating to the magnetic nanoparticles was also successful. However, it is true that with the addition of the silica coating the final structure presented more aggregation. This might be a big inconvenience, as it will become difficult to obtain well separated NPs with gold coating. This was one of the main reasons why, although the hybrid nanostructure built with MUA was performed, the results were not very satisfactory due to NPs show high aggregation and it is not even clear whether the union of both structures was well achieved.

All in all, we conclude that the synthesis and silica coating procedures are under control obtaining the desired results, whereas the combination of both nanoparticles with MUA to build the hybrid nanostrucure needs more research to optimise the procedure and improve its results.

Acknowledgments

I would like to thank my advisor, Dr. Xavier Batlle Gelabert and Mariona Escoda Torroella, both from the group of Magnetic Nanomaterials at Physics Faculty of University of Barcelona, for supervising my work and teach me how to proceed at the laboratory. This work was supported by Spanish MINECO (MAT2015-68772-P), Catalan DURSI (2014SGR220), and European Union FEDER funds (Una manera de hacer Europa). Finally, I would also like to thank my family and friends for all their support.

[1] Pedro Tartaj, Maria del Puerto Morales, Sabino Veintemillas-Verdaguer, Teresita Gonzalez-Carreo and Carlos J. Serna, *The preparation of magnetic nanoparticles for applications in biomedicine* J. Phys. D: Appl. Phys. **36**, R182R197 (2003)

[2] Xiaojun Ji, Ruping Shao, Andrew M. Elliott, R. Jason Stafford, Emilio Esparza-Coss, James A. Bankson, Gan Liang, Zhi-Ping Luo, Keeseong Park, John T. Markert, and Chun Li, *Bifunctional Gold Nanoshells with a Superparamagnetic Iron Oxide-Silica Core Suitable for Both MR Imaging and Photothermal Therapy*, J. Phys. Chem. **111**, 6245-6251 (2007)

[3] S. Narjes Abdollahi, Malek Naderi, Ghasse, Amoabediny, *Synthesis and physicochemical characterization of tunable silica-gold nanoshells via seed growth method*, Colloids and Surface A: Physicochem. Eng. Aspects **414**, 345-351 (2012)

[4] Inmaculada Urries, Cristina Munoz, Leyre Gomez, Clara Marquina,Victor Sebastian, Manuel Arrueboad and Jesus Santamaria *Magneto-plasmonic nanoparticles as theranostic platforms for magnetic resonance imaging, drug delivery and NIR hyperthermia applications*, Nanoscale **6**, 9230 (2014)

[5] Hitesh G. Bagaria, Earl T. Ada, Mohammed Shamsuzzoha, David E. Nikles and Duane T. Johnson, *Understanding Mercapto Ligand Exchange on the Surface of FePt Nanoparticles*, Langmuir **22**, 7732-7737 (2006)

[6] P. de la Presa, T. Rueda, M. P. Morales and A. Hernando, *Ligand exchange in gold-coated FePt nanoparticles*

[7] Carlos Moya, Maria del Puerto Morales, Xavier Batlle and Amilcar Labarta *Turning the magnetic properties of Co-ferrite nanoparticles though 1,2-hexadecanediol concentration in the reaction mixture*, Phys. Chem. Chem. Phys. **17**, 13143 (2015)

[8] Carlos Moya, Xavier Batlle and Amilcar Labarta, *The effect of oleic acid on the synthesis of* $Fe_{3-x}O_4$ *nanoparticles over a wide size range*, Phys. Chem. Chem Phys. **17**, 277373 (2015)

[9] Carla Cannas, Anna Musinu, Andre Ardu, Federica orru, Davide Peddis, Mariano Casu, Roberta Sanna, Fabrizio Angius, Giacomo Diaz and Giorgio Piccaluga, $CoFe_2O_4$ *and* $CoFe_2O_4/SiO_2$ *Core/Shell Nanoparticles: Magnetic and Spectroscopic Study*, Che,. Mater **22**, 3353-3361 3353 (2010)

[10] Carlos Moya Alvarez, *Magnetism in Magnetic Nanoparticles* University of Barcelona (2015)

[11] Vincenzo Amendola, Roberto Pilot, Marco Frasconi, Onofrio M Marago, Maria Antonia Iati, *Surface plasmon resonance in gold nanoparticles: a review*, J. Phys.: Condens. Matter **29** (2017)